Quantum Electronics **48** (4) 390 – 394 (2018) ©2018 Kvantovaya Elektronika and Turpion Ltd

LASERS https://doi.org/10.1070/QEL16586

Power characteristics of lasers with quantum-well waveguides and blocking layers

A.A. Afonenko, D.V. Ushakov, V.Ya. Aleshkin, A.A. Dubinov, N.V. Dikareva, S.M. Nekorkin, B.N. Zvonkov

Abstract. **The power characteristics of lasers with a quantum-well (QW) waveguide are calculated based on a complex model taking into account the diffusion and drift of charge carriers, capture of electrons and holes at the QW levels, spatial distribution of radiation in the cavity, intraband absorption, and heating of the active region. Structures with doped blocking barrier layers are proposed, which allow one to decrease leakage currents to a few percent. The calculated average output power of a laser based on the GaInAs/GaAs QW heterostructure (aperture 100 μm) with a QW waveguide and a GaAsP doped blocking layer in a pulsed regime was 29 W at 80-A current pulses with a duration of 5 μs.**

Keywords: *power characteristics, QW waveguide, potential barriers, diffusion-drift model, intraband absorption, leakage currents, active region heating.*

1. Introduction

The use of a wide dielectric waveguide in high-power semiconductor lasers makes it possible to decrease the load on the mirrors and reduce optical losses [1, 2]. Waveguides in quantum-well (QW) lasers are formed using the difference in the refractive indices of the QW material and the surrounding semiconductor. These lasers are developed based, for example, on InGaAs/InP [3], GaAsSb/GaAs [4], and InGaAs/GaAs [5] systems. In contrast to ultrawide waveguides, the problem of mode selection in QW waveguides is less pronounced because the optical confinement factor for the zero mode localised near the QW is larger than for modes localised between the doped regions (Fig. 1). The main advantage of weak waveguides is a narrower (15 – 20°) directional pattern [3, 5].

One of the factors limiting the output power of lasers with QW waveguides are high leakage currents due to the absence of wide-gap emitters [6]. An effective method to restrict the current and control nonuniform excitation of laser heterostructures is the use of doped wide-gap layers [7 – 9]. For these purposes, it would be preferable to use an undoped heterostructure, which forms a barrier mainly in the conduction band and does not increase internal losses, as it takes place in the case of doping. However, studies [10, 11] revealed a low efficiency of an $Al_{0.42}Ga_{0.38}In_{0.2}As$ layer, which forms a 78-meV barrier for electrons.

In the present work, we propose structures with a QW waveguide with additional doped wide-gap barrier layers blocking leakage of charge carriers and model the power characteristics of these lasers. The problem of using wide-gap layers with a lower refractive index is that they cause an antiwaveguide effect and may lead to disappearance of the weak waveguide.

2. Theoretical model of the laser

The power characteristics were calculated based on a two-dimensional spatial model of the laser. We analysed the distribution of charge carriers, the laser mode intensities, and the temperatures along the cavity axis (x axis) and along the normal to the plane of the layers (z axis, Fig. 1).

The band diagrams and electrophysical characteristics were calculated based on the distributed diffusion-drift model [6], in which the spontaneous recombination rates and the gain coefficients were calculated within the direct-transition model taking into account the spectral broadening effect. The free-carrier absorption coefficient was assumed to be proportional to the concentration of electrons and holes with allowance for the radiation intensity distribution in the waveguide. The radiation power distribution along the cavity was found from the Bouguer equation for the forward and backward waves taking into account the reflectances from the cavity faces. The functional dependences of the gain and free-carrier absorption coefficients on the local photon density and temperature were found using a biquadratic interpolation by nine values of these parameters calculated based on the diffusion-drift model for different temperatures and internal-loss coefficients at a given pump current density.

The change in the active layer temperature $T - T_0$ after switching on the pump current pulse with duration τ was found using the Green function formalism as

$$T(t,x) - T_0 = \int_0^t G_c(\tau) w_{heat}(t-\tau,x)\,d\tau + \int_0^t G_s(\tau) j^2(t-\tau,x)\,d\tau. \quad (1)$$

A.A. Afonenko, D.V. Ushakov Belarussian State University, prosp. Nezavisimosty 4, 220030 Minsk, Belarus; e-mail: afonenko@bsu.by, UshakovDV@bsu.by;
V.Ya. Aleshkin, A.A. Dubinov Institute for Physics of Microstructures, Branch of the Institute of Applied Physics, Russian Academy of Sciences, Akademicheskaya ul. 7, 603087 der. Afonino, Kstovskii raion, Nizhny Novgorod region, Russia; N.I. Lobachevsky State University of Nizhny Novgorod, prosp. Gagarina 23/3, 603950 Nizhny Novgorod, Russia; e-mail: aleshkin@ipmras.ru, sanya@ipm.sci-nnov.ru;
N.V. Dikareva, S.M. Nekorkin, B.N. Zvonkov N.I. Lobachevsky State University of Nizhny Novgorod, prosp. Gagarina 23/3, 603950 Nizhny Novgorod, Russia; e-mail: dnat@ro.ru, zvonkov@nifti.unn.ru

Received 4 December 2017; revision received 30 January 2018
Kvantovaya Elektronika **48** (4) 390 – 394 (2018)
Translated by M.N. Basieva

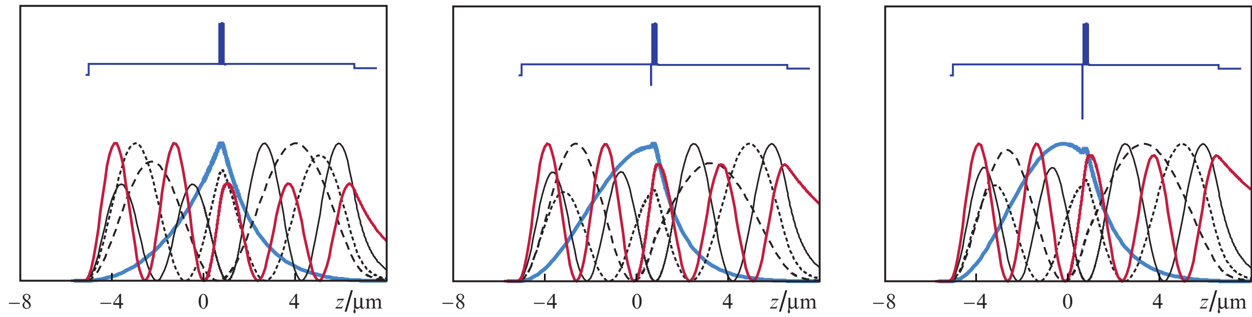

Figure 1. Distributions of mode intensities of laser structures (bottom) with corresponding refractive index profiles (top).

Here, $G_c(\tau)$ and $G_s(\tau)$ are the Green functions for heat sources in the central part of the heterostructure and outside it (for Joule heating);

$$w_{heat}(t,x) = j(t,x)U(t,x) - v_{gr}[g(t,x) - \rho_{int}(t,x)]S(t,x)h\omega(t) \quad (2)$$

is the power of heat sources in the central part of the heterostructure per unit area; $j(t,x)$ and $U(t,x)$ are the current density and voltage at the central part of the structure; $g(t,x)$ is the mode gain; $\rho_{int}(t,x)$ is the internal loss coefficient; $h\omega(t)$ is the laser mode photon energy; $S(t,x)$ is the two-dimensional photon density; and v_{gr} is the group velocity of light in the waveguide.

The Green functions $G_c(\tau)$ and $G_s(\tau)$ for the temperatures of the active layers were found from the numerical solution of the one-dimensional (along the z axis) thermal conductivity equation taking into account the corresponding localisation of heat sources for the structure including all the epitaxial layers, substrate, solder, and heat sink. Heat transfer along the cavity (x axes) was not taken into account. This approach is based on the fact that the effective distance at which heat is transferred from a point source in GaAs during the pulse duration $\tau = 5$ μs is $\sim\sqrt{2\chi\tau} = 22$ μm (χ is the thermal diffusivity). This distance is many times larger than the active region thickness, but is much shorter than the substrate and heat sink thicknesses and the cavity length.

For numerical calculations, we used the band structure parameters and the charge carrier mobilities with allowance for their temperature dependences from [12, 13]. The absorption cross sections for electrons and holes (5×10^{-18} and 10^{-17} cm^2, respectively) were extrapolated form the experimental data [14, 15]. The gain and spontaneous emission spectra were found within a model with the wave vector selection rule [16]. The refractive index was determined by the experimental data of [17] taking into account the contribution from free charge carriers [3] and interband transitions [18].

To test the physical model and the material parameters, we calculated the structure described in [5]. Good agreement with experimental data was obtained for the directional pattern, threshold current, output power, and internal loss coefficient. The calculated leakages were 30%–40% depending on the pump current, which also correlates with the internal quantum yield of stimulated emission estimated in the work (70%).

3. Laser structure design

The first studied structure, as well as all the other structures, consisted of waveguiding layers, formed by six undoped $In_{0.32}Ga_{0.68}As$ QWs 6 nm wide, and GaAs cladding layers 5.6 μm thick doped with p- and n-type impurities with a concentration of 2×10^{17} cm^{-3} (Figs 1 and 2a). The concentration of the n-type dopant in the substrate was 10^{18} cm^{-3}. A p^+-GaAs layer with a dopant concentration of 10^{19} cm^{-3} was positioned between the p-type cladding layer and a metal contact. As a barrier layer blocking the electron leakage in the second structure (Figs 1 and 2b), we additionally used a 20-nm-thick GaAs layer with an acceptor concentration of 2×10^{19} cm^{-3}. To increase the potential barrier in the third structure (Figs 1 and 2c), the central part of the doped block-

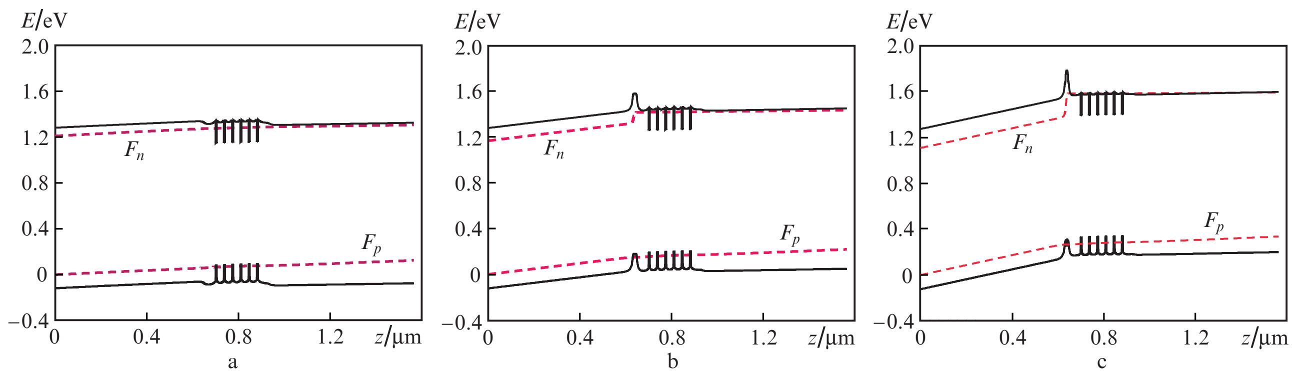

Figure 2. Band diagrams of the central part of laser structures with (a) QW waveguide, (b) doped blocking layer, and (c) doped blocking heterolayer at a current of 125 A and a temperature of 350 K; F_n and F_p are the quasi-Fermi levels for electrons and holes.

Table 1. Parameters of a laser structure with a doped heterobarrier.

Layer number	Layer type	Layer thickness/nm	Doping	Layer material
1	Contact	150	10^{19}	GaAs, *p*-type
2	Waveguide	5630	2×10^{17}	GaAs, *p*-type
3	Barrier	5	2×10^{19}	GaAs, *p*-type
4	Barrier	10	2×10^{19}	$GaAs_{0.9}P_{0.1}$, *p*-type
5	Barrier	5	2×10^{19}	GaAs, *p*-type
6	Spacer	50	–	GaAs, undoped
7	QW	6	–	$In_{0.32}Ga_{0.68}As$, undoped
8	Spacer	30	–	GaAs, undoped
...			pairs of layers 7 and 8 (QW + spacer)	
18	Spacer	20	–	GaAs, undoped
19	Waveguide	5650	2×10^{17}	GaAs, *n*-type
20	Substrate	150000	10^{18}	GaAs, *n*-type

ing layer 10 nm thick was made of $GaAs_{0.9}P_{0.1}$, which has a wider band gap (Table 1). The reflectances of the mirrors were taken to be 95% and 5%; the laser chip length and width were 4 mm and 100 μm, respectively. The calculated laser wavelength was 1.05 μm.

4. Calculation results

For lasers with QW waveguides, it is very important to correctly calculate the refractive index. In the present work, the refractive index was calculated based on the Adachi model [17] modified for quantum-confinement layers. The near-edge absorption contribution was taken into account using the Kramers–Kronig relation. The calculations show that, taking into account the quantum-confinement nature of absorption in a QW, the refractive index in it is lower than in a bulk semiconductor, which is explained by a lower density of states in QW layers and by a shift of the states to higher energies.

The optical confinement factor in the analysed structures (Figs 2a–2c) was, respectively, 0.0018, 0.0015, and 0.0013 per QW. It should be noted that an important feature in a weak waveguide is the dependence of the refractive index on the concentration of electrons and holes in the structure. A higher doping of the substrate and the p^+-GaAs contact layer leads to additional optical confinement. For example, without taking this effect into account, the optical confinement factor in the first structure is 0.0016.

As is seen from the energy band diagrams in Fig. 2, the potential barrier near a QW lowers the quasi-Fermi levels for electrons F_n and decreases the leakage currents. The barrier height can be controlled either by changing the doping level or by adding a layer of a wide-gap material. The potential barriers for the second and third structures at a temperature of 350 K were 150 (Fig. 2b) and 230 meV (Fig. 2c). In both cases, one observes a weakening of the waveguide (due to doping and the presence of a wide-gap material with a lower refractive index). Numerical calculation showed that, in the case of using a $GaAs_{1-x}P_x$ barrier, the optimum phosphorus concentration is 10%.

The laser characteristics were calculated for pumping by rectangular current pulses with a duration of 5 μs. Due to different reflectances of the mirrors, the radiation power distribution along the cavity is strongly inhomogeneous, which affects the longitudinal dependences of the internal loss coefficient and temperature (Fig. 3). Due to heating of the laser diode during the pulse action, the radiation power decreases and the internal loss coefficient increases. The dependences shown in Fig. 4 are averaged over the pulse duration.

At an injection current of about 10 A, the leakage currents in the structure without barrier layers are about 35%, which corresponds to the internal quantum yield of stimulated emission close to the yield measured for a structure with a similar design (70%) [5] (Fig. 4). The introduction of a blocking layer leads to a considerable decrease in electron leakage currents,

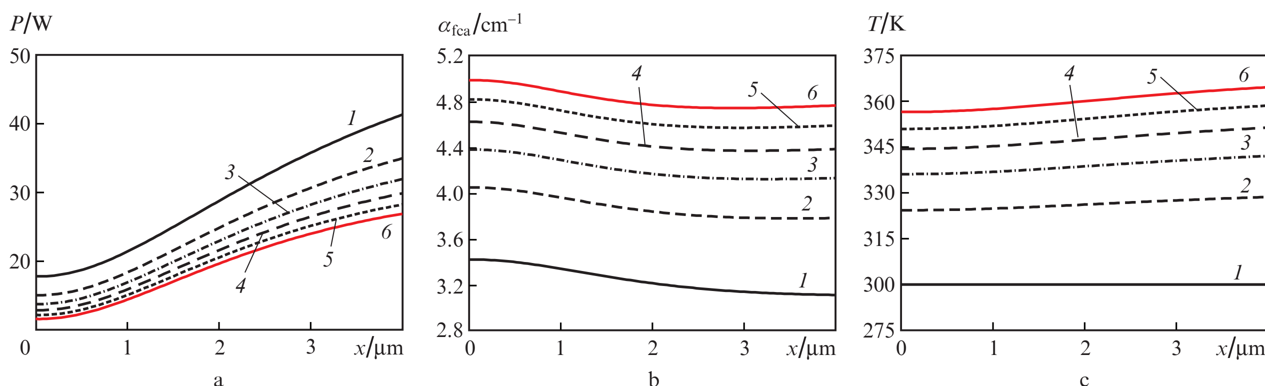

Figure 3. Space–time dependences of (a) laser power P, (b) free-carrier absorption coefficient α_{fca}, and (c) active region temperature T for a structure with doped blocking heterolayers at a current of 90 A. Curves (*1*, *2* ..., *6*) correspond to time instants of 0, 1, ..., 5 μs.

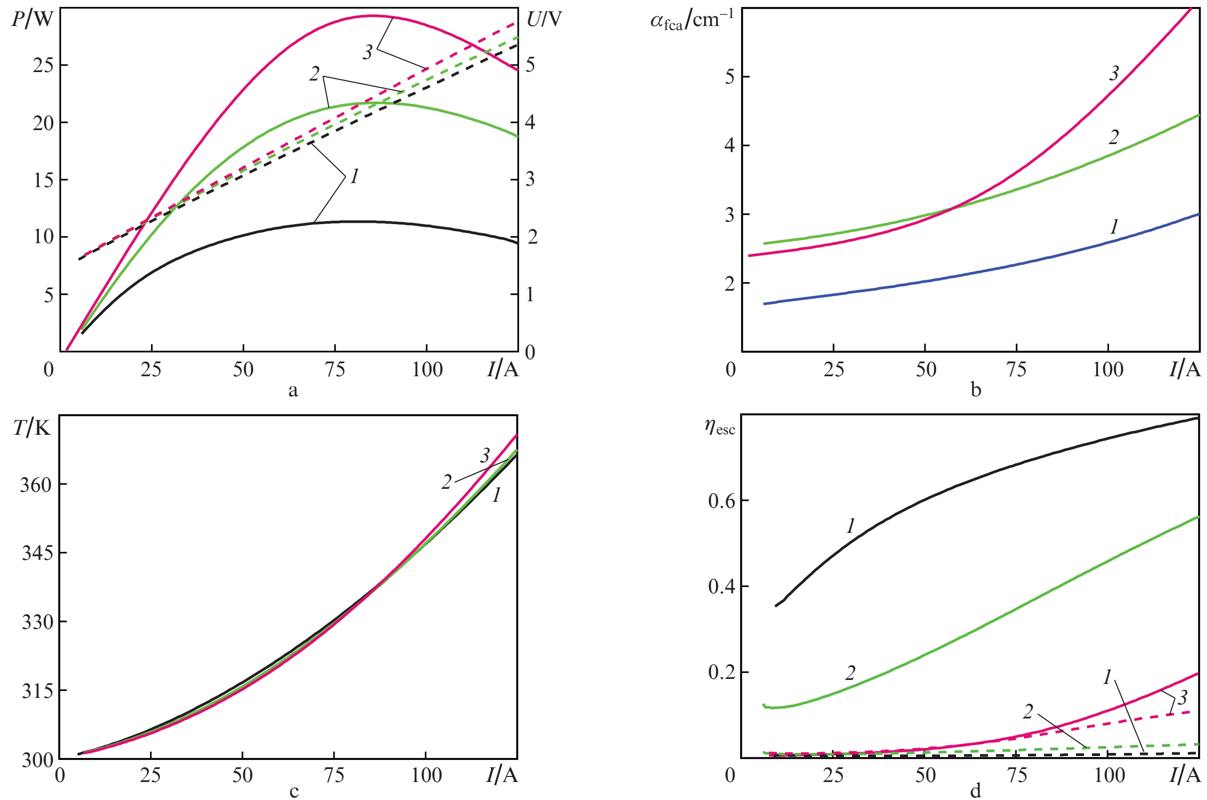

Figure 4. (a) Pulse-average laser power (solid curves) and voltage applied to the structure (dashed lines); (b) average free-carrier absorption coefficient; (c) average active region temperature; and (d) fractions of electron (solid curves) and hole (dashed curves) leakage currents η_{esc} for lasers with six QWs upon pumping by 5-μs pulses for structures (*1*) without blocking layers, (*2*) with doped blocking layers, and (*3*) with doped blocking heterolayers.

namely, from 69% at a current of 80 A for ordinary QW lasers to 5% for lasers with a doped blocking heterolayer. In this case, due to doping of the blocking layer, the free-carrier absorption coefficient increases approximately by 1 cm^{-1}, but still remains rather low. A decrease in the leakage currents allows an increase in the maximum laser power. At a current of 80 A, the calculated average power of a laser with a doped blocking heterolayer increases by a factor of 2.5 and may reach 29 W. This is comparable with the characteristics of high-power leaky-mode lasers [19]. The calculations were performed for the optimum cavity length $L = 4$ mm, at which the internal losses at the maximum power are close to the external cavity losses (3.8 cm^{-1}). The doping level of the cladding layers (2×10^{17} cm^{-3}) is also optimal for obtaining the maximum power. An increase in doping leads to an increase in the internal losses, while the ohmic resistance and the active region heating increase with deceasing doping.

The existence of potential barriers almost does not affect the temperature of the active region of the structure shown in Fig. 2c. A decrease in heating of the structure due to the extraction of a higher radiation power [formula (2)] competes with an increase in the voltage at the structure (see Fig. 2) caused by an increase in the effective ohmic resistance with decreasing electron leakage currents. The calculated maximum voltage difference was 0.3 V at a current of 125 A. The series resistance of the structure layers was 0.026–0.029 Ω (Fig. 4a).

As is seen from Fig. 4d, the calculated fraction of hole leakage currents at a current of 80 A is 6%. To efficiently block the hole transport, it is necessary to form barriers in the valence band similar to the barriers in the conduction band. To prevent deterioration of the waveguiding properties, one could decrease barriers in the conduction band, but this is unreasonable because the electron leakage currents are dominant. Calculations showed that the existence of a 72-meV barrier in the valence band (doping with donors with a concentration of 2×10^{18} cm^{-3}) almost does not decrease the hole leakage.

It should be noted that the introduction of blocking layer leads to a nonuniform distribution of electrons in waveguiding layers before and after the QW. Therefore, due to the dependence of the refractive index on the charge carrier concentration, which is more pronounced for electrons than for holes, the waveguide symmetry is disturbed (see Fig. 1), the mode begins to localise mainly on the p-emitter side, and the directional pattern width increases with increasing pump current. At the same time, estimates show that the directional pattern width at half power in the plane perpendicular to the p–n junction remains small (does not exceed 10°).

Thus, in the present work we have developed a numerical model of a semiconductor injection laser, which additionally takes into account the free-carrier absorption, heating of the structure, spatial distribution of laser radiation in the cavity, and the effect of size quantisation on the refractive index of QW layers. Laser structures with a QW waveguide are analysed based on the developed model. It is shown that the introduction of a doped blocking layer (in particular, a heterolayer) makes it possible to form an efficient potential barrier for minority charge carriers, decrease leakage currents, and increase the laser power. According to calculations, the aver-

age power of a laser (with an aperture of 100 μm) based on a GaInAs/GaAs QW heterostructure with a QW waveguide and a GaAsP blocking layer may reach 29 W at a current of 80 A and a pump pulse duration of 5 μs. The directional pattern width in the plane perpendicular to the p–n junction is estimated to be no larger than 10°.

Acknowledgements. This work was supported by the Belorussian Republican Foundation for Basic Research [Project BRFBR–RFBR No. F16R-018 (16-52-00049)] and by the Grant of the President of the Russian Federation for young scientists and postgraduate students performing advanced research and development in priority areas of modernisation of the Russian Economics (Project No. SP-109.2016.3).

References

1. Gelovani V.A., Skorokhodov A.P., Shveikin V.I. *Vysokoeffektivnye vysokomoshchnye diodnye lasery novogo tipa* (High-Efficiency High-Power New-Type Diode Lasers) (Moscow: USRR, 2005).
2. Slipchenko S.O., Sokolova Z.N., Pikhtin N.A., Borshchev K.S., Vinokurov D.A., Tarasov I.S. *Fiz. Tekh. Poluprovodn.*, **40**, 1017 (2006).
3. Aleshkin V.Ya., Dikareva N.V., Dubinov A.A., Zvonkov B.N., Karzanova M.V., Kudryavtsev K.E., Nekorkin S.M., Yablonskii A.N. *Quantum Electron.*, **43**, 401 (2013) [*Kvantovaya Elektron.*, **43**, 401 (2013)].
4. Aleshkin V.Ya., Afonenko A.A., Dikareva N.V., Dubinov A.A., Kudryavtsev K.E., Morozov S.V., Nekorkin S.M. *Fiz. Tekh. Poluprovodn.*, **47**, 1486 (2013).
5. Slipchenko S.O., Podoskin A.A., Pikhtin N.A., Leshko A.Yu., Rozhkov A.V., Tarasov I.S. *Pis'ma Zh. Tekh. Fiz.*, **39**, 9 (2013).
6. Afonenko A.A., Ushakov D.V. *Fiz. Tekh. Poluprovodn.*, **48**, 88 (2014).
7. Afonenko A.A., Kononenko V.K., Manak I.S. *Izv. Ross. Akad. Nauk, Ser. Fiz.*, **65**, 227 (2001).
8. Ushakov D.V., Kononenko V.K. *Quantum Electron.*, **38**, 1001 (2008) [*Kvantovaya Elektron.*, **38**, 1001 (2008)].
9. Veselov D.A., Shashkin I.S., Bakhvalov K.V., Lyutetskii A.V., Pikhtin N.A., Rastegaeva M.G., Slipchenko S.O., Bechvai E.A., Strelets V.A., Shamakhov V.V., Tarasov I.S. *Fiz. Tekh. Poluprovodn.*, **50**, 1247 (2016).
10. Marmalyuk A.A., Ryaboshtan Yu.L., Gorlachuk P.V. *Quantum Electron.*, **47**, 272 (2017) [*Kvantovaya Elektron.*, **47**, 272 (2017)].
11. Polubavkina Yu.S., Zubov F.I., Moiseev E.I., Kryzhanovskaya N.V., Maksimov M.V., Semenova E.S., Yvind K., Asryan L.V., Zhukov A.E. *Fiz. Tekh. Poluprovodn.*, **51**, 263 (2017).
12. Vurgaftman I., Meyer J.R., Ram-Mohan L.R. *J. Appl. Phys.*, **89**, 5815 (2001).
13. Palankovski V., Quay R. *Analysis and Simulation of Heterostructure Devices* (Wien, New York: Springer, 2004).
14. Spitzer W.G., Whelan J.M. *Phys. Rev.*, **114**, 59 (1959).
15. Rinzan M.B.M., Esaev D.G., Perera A.G.U., Matsik S.G., Von Winckel G., Stintz A., Krishna S. *Appl. Phys. Lett.*, **85**, 5236 (2004).
16. Ushakov D.V., Afonenko A.A., Aleshkin V.Ya. *Quantum Electron.*, **43**, 999 (2013) [*Kvantovaya Elektron.*, **43**, 999 (2013)].
17. Adachi S. *Phys. Rev. B*, **35**, 7454 (1987).
18. Afonenko A.A., Manak I.S. *Elektromagnitnaya teoriya poluprovodnikovykh laserov* (Electromagnetic Theory of Semiconductor Lasers) (Minsk: Belarusian State University, 1997).
19. Nekorkin S.M., Zvonkov B.N., Baidus' N.V., Dikareva N.V., Vikhrova O.V., Afonenko A.A., Ushakov D.V. *Fiz. Tekh. Poluprovodn.*, **51**, 75 (2017).